The current issue and full text archive of this journal is available at
www.emeraldinsight.com/0961-5539.htm

Received 13 July 2004
Revised 4 October 2007
Accepted 4 October 2007

Conjugate forced convection flow past a circular cylinder with internal heat generation in a porous medium

Nur F. Abd Kadir and D.A.S. Rees
Department of Mechanical Engineering, University of Bath, Bath, UK, and
Ioan Pop
Faculty of Mathematics, University of Cluj, Cluj, Romania

Abstract

Purpose – The aim is to determine the effect of different conductivity ratios on forced convection past a circular cylinder embedded in a porous medium, where the solid cylinder forms a uniform heat source.

Design/methodology/approach – The authors employ an unsteady finite difference method to obtain the resulting steady-state solutions. Interface conditions are applied using the fictitious point method.

Findings – It is found that, the thermal field within the cylinder and in the external porous region depend strongly on the ratio of the respective conductivities. In the extreme cases the cylinder acts either as one with a uniform temperature (high-cylinder conductivity) or with a uniform heat flux (low-cylinder conductivity).

Research limitations/implications – Conductivity ratios in the range $0.1 \leq \gamma \leq 100$ and Péclet numbers in the range, $1 \leq Pe \leq 1,000$ were taken.

Originality/value – Forced convection studies usually focus on cases where the solid phase has a prescribed temperature or heat flux. The present paper employs a uniform heat generation within the cylinder to determine how the therrmal field depends on the Péclet number and the conductivity ratio.

Keywords Heat transfer, Convection, Porous materials, Flow

Paper type Research paper

Nomenclature

C_p = specific heat
f = buffer region function
k = conductivity
K = permeability
p = pressure
Pe = Péclet number
q''' = strength of heat source
r = radial coordinate
R = radius of cylinder
T = dimensional temperature
u = radial velocity
U = free stream velocity
v = angular velocity

Greek characters
γ = conductivity ratio
ψ = streamfunction
ρ = density

One of the authors (IP) wishes to thank the Royal Society for partial financial support. The authors would like to thank one of the referees for making them aware of the paper by Kimura and Yoneya.

International Journal of Numerical Methods for Heat & Fluid Flow
Vol. 18 No. 6, 2008
pp. 730-744

0961-5539
DOI 10.1108/09615530810885542

μ = dynamic viscosity
ϕ = angular coordinate
θ = non-dimensional temperature

Subscripts, superscripts
$-$ = dimensional quantity
c = cylinder
i = grid point index in r-direction
j = grid point index in ϕ-direction
n = timestep
pm = porous medium

Introduction

The importance of heat transfer phenomena associated with free or forced convection flow in porous media is well known. Interest in this area has been motivated by such diverse engineering problems as geothermal energy extraction, storage of nuclear waste material, ground water flows, pollutant dispersion in aquifers, design of nuclear reactors, solar power collectors, compact heat exchangers, food industries, to name just a few applications. The archival publications of transport phenomena in porous media have been reviewed and presented in the recent books by Ingham and Pop (1998, 2002, 2005), Nield and Bejan (2005), Vafai (2000, 2005), Pop and Ingham (2001), Bejan and Kraus (2003), Ingham *et al.* (2004) and Bejan *et al.* (2004).

To date few studies exist of forced convection past a heated cylinder embedded in a porous medium. In a seminal paper Pop and Yan (1998) showed that, it is possible to reduce the high-Péclet number (*Pe*) forced convection problem to self-similar boundary layer form, for which analytical solutions are available. An earlier paper by Nasr *et al.* (1994) looked in detail at how the conductivities and grain sizes of the surrounding porous medium affected heat transfer from a hot cylinder. Kimura (1989) has considered the transient case where the temperature of the cylinder is raised suddenly from the ambient value, and the same author studied an elliptic cylinder using both integral and numerical techniques (Kimura, 1988). More recently, Rees *et al.* (2003) and Wong *et al.* (2004) have considered the effect of utilising the two-temperature model of conduction in a porous medium, where separate but coupled temperature fields associated with the solid and fluid phases are considered; these papers consider both the boundary layer limit ($Pe \rightarrow \infty$) and moderate values of *Pe.* At present, there exists only one paper considering forced convection past a cylinder with a uniform heat flux from its surface. Kimura and Yoneya (1992) conducted an experimental study of this configuration and presented the result of an approximate analytical study of the boundary layer which arises at high-Péclet number boundary. Therefore, at the present time, there are are no published studies containing detailed moderate Péclet number computations or a rigorous high-Péclet number boundary layer analysis.

Forced convection flows usually involve heated boundaries with either a prescribed surface temperature or surface heat flux. A somewhat different situation is considered here where uniform internal heat generation within a solid cylinder is the source of heating for the system and where a uniform external flow exists in the porous medium outside of the cylinder. Therefore, this is a type of conjugate heat transfer problem where neither the local surface temperature nor the heat flux at the surface of the cylinder is known in advance. These need to be obtained as part of the numerical solution procedure by imposing continuity of both temperature and heat flux at the surface of the cylinder, as was done by Kimura and Pop (1992) in a free convection problem. Some aspects of the thermal coupling between a solid medium and a neighbouring saturated porous medium and a list of references on the topic may be found in the review articles by Kimura *et al.* (1997) and Pop and Nakayama (1999), and also in the recent papers by

Vaszi *et al.* (2003, 2004). Our aim is, therefore, to determine the behaviour of the thermal field surrounding and within a uniformly heat-generating cylinder which is embedded within a fluid-saturated porous medium with a uniform free stream.

Governing equations

The governing equations for forced convection flow past a circular cylinder of radius R which is embedded in a porous medium are based on the conservation of mass, momentum and thermal energy. We will assume that flow in the porous medium is governed by Darcy's law, and therefore modifications such as form drag (the Forchheimer terms), boundary effects (the Brinkman terms) and anisotropy are either negligible or absent.

With this in mind the equation of continuity and the momentum (Darcy) equations may be written in the forms:

$$\frac{\partial \overline{ru}}{\partial \bar{r}} + \frac{\partial \bar{v}}{\partial \phi} = 0, \tag{1}$$

$$\bar{u} = -\frac{K}{\mu}\,\frac{\partial \bar{p}}{\partial \bar{r}}, \quad \bar{v} = -\frac{K}{\mu}\,\frac{1}{r}\,\frac{\partial \bar{p}}{\partial \phi}, \tag{2a, b}$$

where $\bar{r}$ and ϕ are the radial and angular coordinates and $\bar{u}$ and $\bar{v}$ are the corresponding fluid seepage velocities. The constants, K and μ, are the permeability of the saturated medium and the dynamic viscosity, respectively. The thermal energy equation for the porous medium may be written in the form:

$$k_{\mathrm{pm}}\left[\frac{\partial^2 T_{\mathrm{pm}}}{\partial \bar{r}^2} + \frac{1}{\bar{r}}\,\frac{\partial T_{\mathrm{pm}}}{\partial \bar{r}} + \frac{1}{\bar{r}^2}\,\frac{\partial^2 T_{\mathrm{pm}}}{\partial \phi^2}\right] = (\rho C_p)\left[\bar{u}\frac{\partial T_{\mathrm{pm}}}{\partial \bar{r}} + \frac{\bar{v}}{\bar{r}}\,\frac{\partial T_{\mathrm{pm}}}{\partial \phi}\right], \tag{3}$$

where k_{pm} is the thermal conductivity of the porous medium and T_{pm} its temperature. The values ρ and C_p refer to the density and the specific heat. Likewise, the thermal energy equation for the solid cylinder is:

$$k_{\mathrm{c}}\left[\frac{\partial^2 T_{\mathrm{c}}}{\partial \bar{r}^2} + \frac{1}{\bar{r}}\,\frac{\partial T_{\mathrm{c}}}{\partial \bar{r}} + \frac{1}{\bar{r}^2}\,\frac{\partial^2 T_{\mathrm{c}}}{\partial \phi^2}\right] + q''' = 0. \tag{4}$$

Here, k_{c} is the conductivity of the solid cylinder, q''' is the constant rate of heat production within the cylinder and T_{c} is its temperature.

The cylinder occupies the region $\bar{r} \leq R$ and this provides a natural lengthscale. There is a uniform free stream far from the surface of magnitude U which is in the direction of increasing $\bar{r}$ on $\phi = 0$. Therefore, we choose to non-dimensionalise using the following transformations:

$$\bar{r} = Rr, \quad (\bar{u}, \bar{v}) = U(u, v), \quad \bar{p} = \frac{UR\mu}{K}\,p \quad \text{and} \quad T = T_\infty + \frac{q'''R^2}{k_{\mathrm{c}}}\,\theta, \tag{5}$$

where T_∞ is the constant temperature of the free stream. As the flow is two-dimensional it is convenient to introduce the streamfunction, ψ, according to:

$$u = \frac{1}{r}\,\frac{\partial \psi}{\partial \phi}, \quad v = -\frac{\partial \psi}{\partial r}, \tag{6}$$

and therefore the governing equations (2)-(4), take the non-dimensional form:

$$\frac{\partial^2\psi}{\partial r^2}+\frac{1}{r}\,\frac{\partial\psi}{\partial r}+\frac{1}{r^2}\,\frac{\partial^2\psi}{\partial\phi^2}=0, \tag{7}$$

$$\frac{1}{Pe}\left[\frac{\partial^2\theta_{\mathrm{pm}}}{\partial r^2}+\frac{1}{r}\,\frac{\partial\theta_{\mathrm{pm}}}{\partial r}+\frac{1}{r^2}\,\frac{\partial^2\theta_{\mathrm{pm}}}{\partial\phi^2}\right]=\frac{1}{r}\left[\frac{\partial\psi}{\partial\phi}\,\frac{\partial\theta_{\mathrm{pm}}}{\partial r}-\frac{\partial\psi}{\partial r}\,\frac{\partial\theta_{\mathrm{pm}}}{\partial\phi}\right],\quad (r\geq 1), \tag{8}$$

and:

$$\frac{\partial^2\theta_{\mathrm{c}}}{\partial r^2}+\frac{1}{r}\,\frac{\partial\theta_{\mathrm{c}}}{\partial r}+\frac{1}{r^2}\,\frac{\partial^2\theta_{\mathrm{c}}}{\partial\phi^2}+1=0.\quad (r\leq 1), \tag{9}$$

while the dimensionless form of equation (1) is satisfied by equation (6). The Péclet number, Pe which appears in equation (8) is defined as:

$$Pe=\frac{UR(\rho C_p)}{k_{\mathrm{pm}}}. \tag{10}$$

Equation (7) has the solution:

$$\psi=\left[r-\frac{1}{r}\right]\sin\phi, \tag{11}$$

which yields a uniform free stream of unit magnitude when r is large, and which gives $\psi=0$ on both the axis ($\phi=0,\ \pi$) and the surface of the cylinder ($r=1$).

The boundary conditions for the temperature field are:

- that θ decays to zero as r increases indefinitely; and
- that there is continuity of both temperature and heat flux at the interface between the cylinder and the porous medium.

Therefore, we require:

$$\theta_{\mathrm{c}}=\theta_{\mathrm{pm}}\ \text{ and }\ k_{\mathrm{c}}\frac{\partial\theta_{\mathrm{c}}}{\partial r}=k_{\mathrm{pm}}\frac{\partial\theta_{\mathrm{pm}}}{\partial r}\quad\text{at }\ r=1. \tag{12}$$

Finally, we define the parameter γ, the ratio of the conductivity of the cylinder to that of the porous medium, as, $\gamma=k_{\mathrm{c}}/k_{\mathrm{pm}}$.

Numerical method

Equations (8) and (9) were solved by converting them into time-evolution equations and time-marching to steady state. Thus, the equations solved were:

$$\frac{\partial\theta_{\mathrm{pm}}}{\partial t}=\frac{1}{Pe}\left[\frac{\partial^2\theta_{\mathrm{pm}}}{\partial r^2}+\frac{1}{r}\,\frac{\partial\theta_{\mathrm{pm}}}{\partial r}+\frac{1}{r^2}\,\frac{\partial^2\theta_{\mathrm{pm}}}{\partial\phi^2}\right]-\frac{1}{r}\left[\frac{\partial\psi}{\partial\phi}\,\frac{\partial\theta_{\mathrm{pm}}}{\partial r}-\frac{\partial\psi}{\partial r}\,\frac{\partial\theta_{\mathrm{pm}}}{\partial\phi}\right], \tag{13}$$

and:

$$\frac{\partial \theta_c}{\partial t} = \frac{\partial^2 \theta_c}{\partial r^2} + \frac{1}{r}\frac{\partial \theta_c}{\partial r} + \frac{1}{r^2}\frac{\partial^2 \theta_c}{\partial \phi^2} + 1, \tag{14}$$

where the expressions involving ψ in equation (13) may be expanded using the definition of ψ in equation (11). Equations (13) and (14) were solved using a finite difference method on a uniform grid. We define the radial and angular steplengths as h_r and h_ϕ, respectively, and the number of steps in each of these directions are N_r and N_ϕ. Therefore, $r_i = ih_r$ and $\phi_j = jh_\phi$, define the spatial grid, and the interface is at $i = I$, that is, $I_{hr} = 1$. The time variable is discretised in the same way with the uniform timestep h_t, and discrete values of t being given by $t_n = nh_t$. Finally, the numerical approximation to the exact value of $\phi(r_j, \theta_j, t_n)$ is denoted by θ_{ij}^n.

The governing equations were discretised using standard second order central differences in space, while timestepping was achieved using the DuFort-Frankel method. As the equations are linear, there is no possibility of physical instability, and convergence to an ultimate steady-state is always obtained when the timestep is sufficiently small, otherwise numerical instability arises. On the axis, $\phi = 0, \pi$, central differences in space were employed using the ghost point technique (i.e. setting $\theta_{i,-1}^n = \theta_{i,1}^n$) to ensure even symmetry ($\partial\theta/\partial\phi = 0$), thereby reducing the computational effort.

At the origin it is not possible to discretise equations (13) and (14) directly since some of the coefficients are singular. The Laplacian in equation (14) was therefore approximated using the formula:

$$\frac{1}{h_r^2}\frac{2}{N_\phi}\left[\theta_{c1,0} + 2\sum_{j=1}^{N_\phi - 1}\theta_{c1,j} + \theta_{c1,N_\phi} - 2N_\phi\theta_{c0,0}\right]. \tag{15}$$

Expression (15) may be derived by recourse to standard five-point Cartesian formula with steplengths both equal to h_r, where all possible ways of writing the five-point formula (i.e. by rotating the artesian axes so that axes coincide with the grid-lines ϕ = constant) are averaged, and then modified according to the fact that $\partial\theta_c/\partial\phi = 0$ on the axis.

At the interface not only is the temperature distribution continuous as r increases, but so is the heat flux, as given by equation (11). A straightforward central difference approximation of equation (11) based at the interface will yield an algebraic equation involving a θ_{pm} value at $r = r_{I-1}$ and a θ_c value at $r = r_{I+1}$, both of which may be termed ghost points since they are outside their appropriate domains of existence. However, we may also write down the central difference approximations to both equations (8) and (9) at the interface. Both the resulting expressions contain the two ghost points, and may be added together in a suitable way so that the application of the approximation to equation (11) removes the ghost points from the resulting expression. In this way, we obtain a rather lengthy formula which applies at the interface and which does not contain ghost points.

Finally, we paid attention to possible numerical difficulties associated with the outflow boundary, which occupies that part of the $r = r_{max}$ gridline in the range $0 \le \phi \le 1/2\pi$. Two different ways of treating this boundary were attempted: in Method I we set $\partial\theta_{pm}/\partial r = 0$, while for Method II we used a form of buffer region which damps out thermal disturbances. The latter was inspired by the example of

Kloker *et al.* (1993) who were concerned with the passage out of the computational domain of highly detailed and evolving instabilities to the Blasius boundary layer flow over a flat plate. These authors found that more naive formulations, such as our Method I, cause spatial oscillations which propagate upstream and eventually contaminate the whole flow. They also found that the use of buffer region which damps out disturbances to the basic flow eliminates these unphysical oscillations, and, very importantly, also has an almost negligible upstream effect. For the present paper we employed the buffer region methodology in the following form. At each timestep a new temperature field is determined; if this is notated by $\theta_{i,j}^{n,\mathrm{basic}}$, then the field which is used for subsequent computation is given by:

$$\theta_{i,j}^{n} = f(r_i)\theta_{i,j}^{n,\mathrm{basic}}, \tag{16}$$

where the buffer function, $f(r_i)$, is unity when $r_i < 0.8{*}r_{\max}$, but takes the values:

$$f(r_i) = \cos^2\left[\left(\frac{5r_i}{r_{\max}} - 4\right)\frac{\pi}{2}\right]. \tag{17}$$

This form for $f(r_i)$ allows the "disturbance" (i.e. the developing thermal field) to be brought smoothly down to zero at outflow. Extensive tests were undertaken to verify whether or not a larger buffer region is necessary, and to determine how large the computational domain should be in the radial direction that the results we present below are independent of the size and extent of the computational and buffer regions. It as found not only that the buffer domain can safely be as small as 20 per cent of the computational domain, but also the results were also found to coincide almost exactly with those obtained using Method I, the naive approach to treating the outflow boundary. Therefore, we conclude that the modelling of outflow boundaries in porous media is more robust than those involving clear fluids.

The code we developed used either a zero temperature field as the initial condition, or a previously converged solution for the same parameter case on a coarser grid, which was then interpolated onto the given grid; this latter approach was found to yield much improved convergence times on relatively fine grids. Convergence itself was deemed to have occurred when the maximum absolute change in either θ_{pm} or θ_{c} over one timestep is less than 10^{-8}. In general, we found that the required extent of the computational domain depends strongly on the magnitude of Pe, and only slightly on the value of γ. Details of the values of $r_{\max}$ and the number of grid points may be found in Table I. In practice, we solved the governing equations three times for each parameter set; for $Pe = 1{,}000$, for example, the three solutions were on grids with

Pe	h_t	$r_{\max}$	$N_r \times N_\phi$
1,000	0.001	2.5	240 × 240
300	0.001	5	240 × 240
100	0.001	5	240 × 240
30	0.002	8	256 × 256
10	0.005	5	240 × 240
3	0.005	15	240 × 240
1	0.005	25	300 × 240

Table I.
Details of the grids used for each value of Pe

60 × 60, 120 × 120 and 240 × 240 points, where all figures were prepared using the solution on the finest grid.

Results and discussion

The detailed temperature field within the cylinder and the external porous medium are dependent on the two parameters, Pe and γ. Figures 1-3 show how the isotherms, axis temperature and cylinder surface temperature vary with Pe while $\gamma = 1$. The region within which the temperature field is significantly different from zero is seen clearly in Figure 1 to decrease substantially as the strength of the external flow, as measured by the Péclet number, Pe, increases. At small values of Pe heat is able to conduct fairly readily upstream of the cylinder, but, when Pe becomes large, the thermal field within the porous medium is confined to a boundary layer on the surface of the cylinder, and to the thermal wake downstream of the cylinder. For this particular value of γ, for which the conductivity ratio of the cylinder to that of the porous medium is unity, the temperature distribution within the cylinder itself is roughly parabolic in r.

The above observations regarding the thermal field may also be shown in Figure 2 which displays the temperature on the central axis (i.e. on $\phi = 0$, which corresponds to

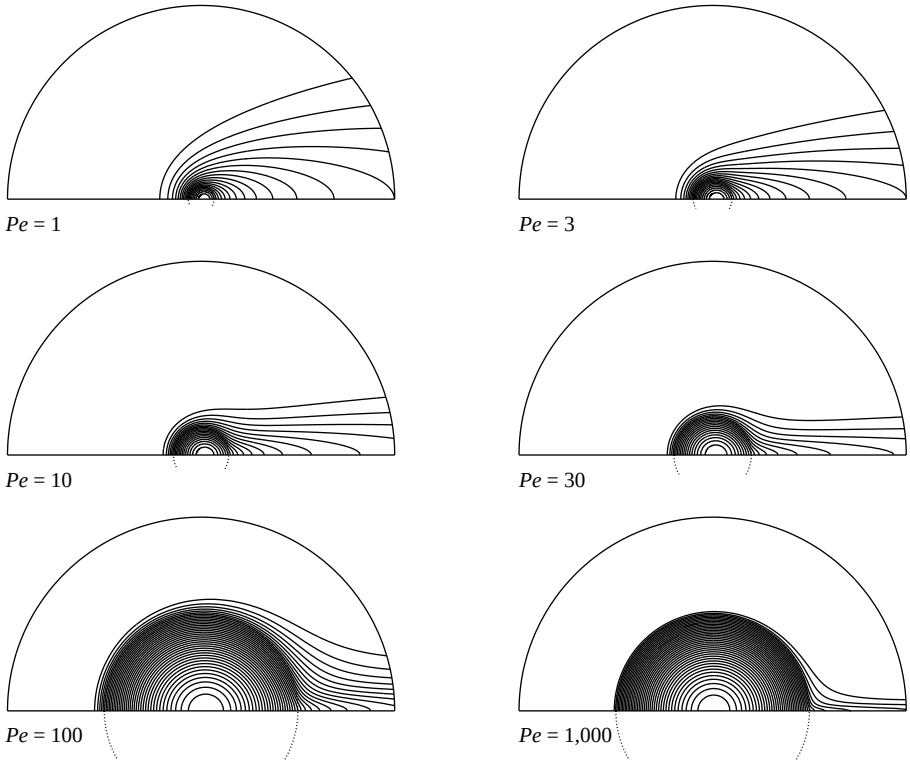

Figure 1.
The effect of different values of the Péclet number Pe, on the isotherms for $\gamma = 1$

Notes: Isotherms are spaced using 40 equal intervals between zero and the maximum temperature for each case and the dotted line indicates the location of the surface of the heated cylinder, these conventions also apply to Figures 4 and 7

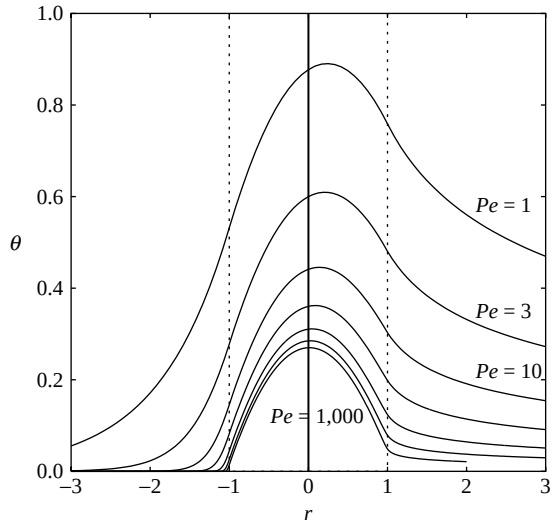

Notes: The positions of the interface between the cylinder and the porous medium are shown by the dashed line

Figure 2.
Temperature profiles along the axis of the cylinder in the direction of the external free stream for $\gamma = 1$ and for $Pe = 1$, 3, 10, 100, 300, and 1,000

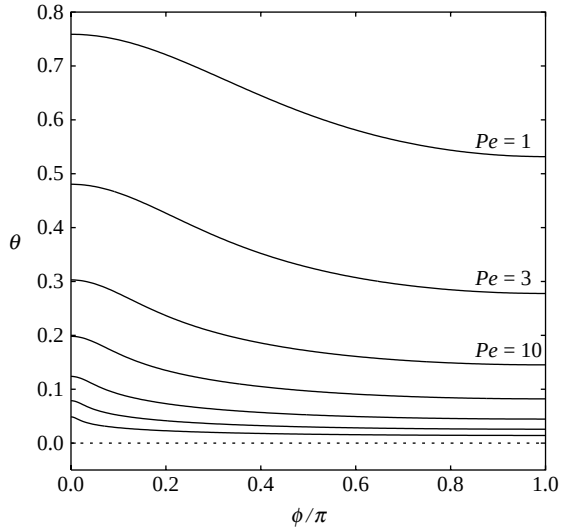

Notes: The parameters are given by $\gamma = 1$ and Pe = 1, 3, 10, 30, 100, 300 and 1,000. The dashed line denotes the horizontal axis

Figure 3.
Non-dimensional temperature profiles along the surface of the cylinder from the rear stagnation point at $\phi = 0$ to the forward stagnation point at $\phi/\pi = 1$

positive values of r in this figure, and on $\phi = \pi$ for negative values of r). Whilst Figure 1 shows isotherms using 40 intervals between zero and the maximum temperature achieved, Figure 2 shows the absolute temperatures as functions of both r and Pe. For low values of Pe the maximum temperature achieved is higher than for large values of Pe – this is due to the increased rapidity with which heat is transported

away from the cylinder. However, given that the heat source within the cylinder is uniform and constant, the temperature gradients at $r = \pm 1$, as shown in Figure 2 as the temperature curves cross the dashed lines, vary only slightly with *Pe*. The detailed surface temperature variation with ϕ for different values of *Pe* are shown in Figure 3. For small values of *Pe* the relative variation in the non-dimensional temperature, θ is not large, but for large values of *Pe*, there is a relatively large rise in ϕ close to the rear stagnation point at $\phi = 0$. This suggests that, a large *Pe* asymptotic analysis might proceed, at least initially, by assuming a sufficiently small amplitude parabolic temperature profile within the cylinder; it is hoped to report on such an analysis in the future.

Now we turn to the effects of varying the conductivity ratio, γ. Figures 4-6 are concerned with these effects for $Pe = 100$, which is fairly typical for a high-Péclet number flow, while Figures 7-9 correspond to $Pe = 1$.

Figure 4 shows isotherms for the $Pe = 100$ case for a variety of values of γ. When γ is large, which corresponds to the cylinder having a very high conductivity, then there is little variation in the temperature profile within the cylinder, due to the fact that heat is transported easily through the solid medium. For such a highly conducting cylinder the maximum temperature it attains is located increasingly close to the rear stagnation point as γ increases, as may be shown in Figure 5, and the maximum temperature attained also increases due to the increased heat capacity of the cylinder.

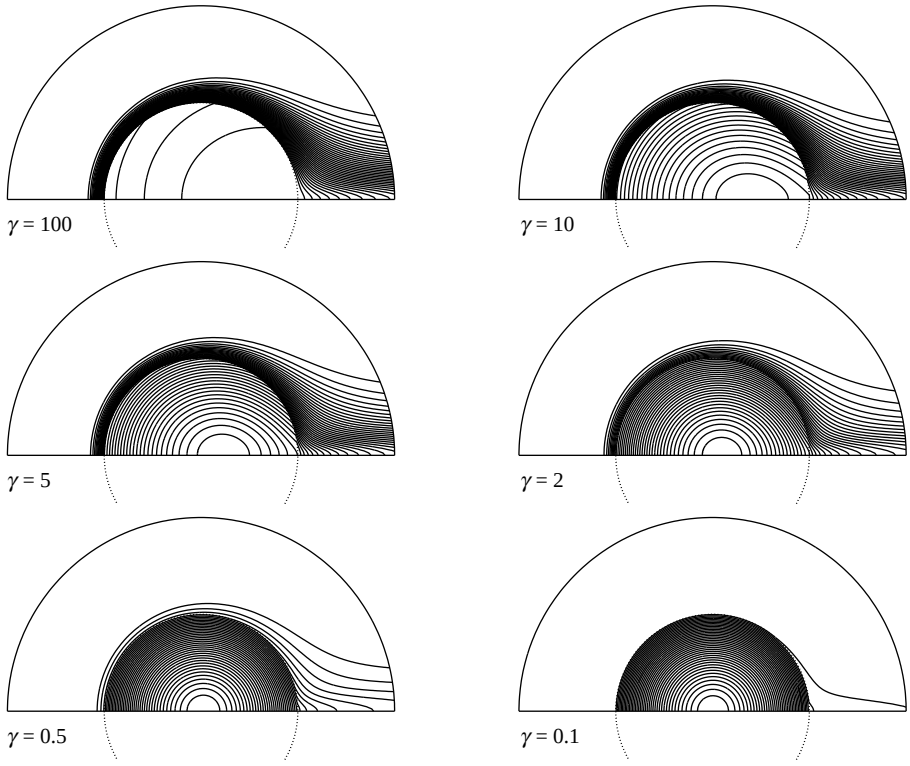

Figure 4.
The effect of different values of the conductivity ratio γ on the isotherms for $Pe = 100$

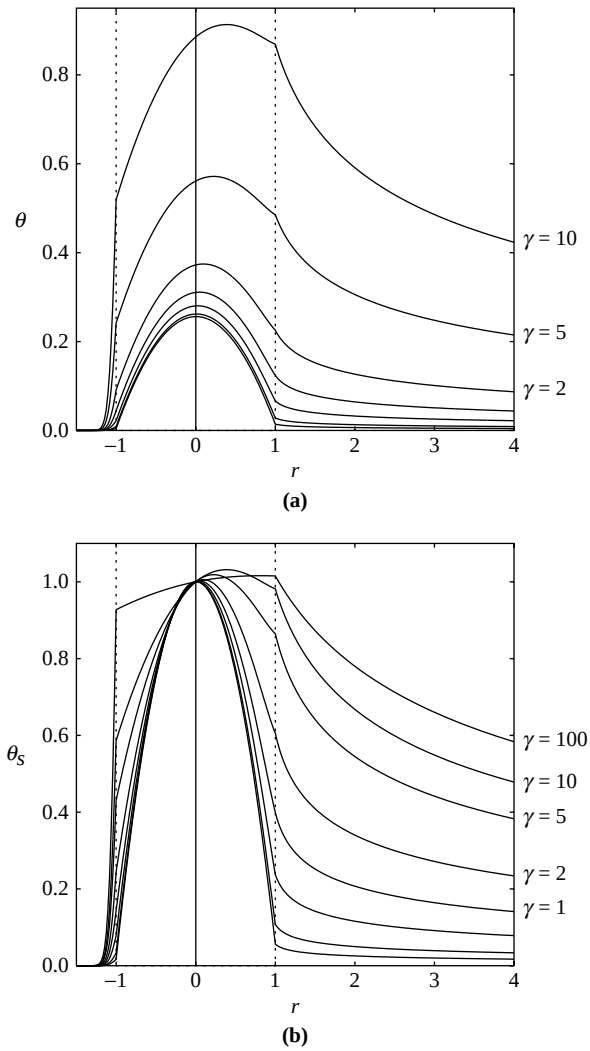

Notes: (a) computed temperature profiles; (b) scaled temperature profiles, θ_S (which also includes $\gamma = 100$)

Figure 5.
Non-dimensional temperature profiles along the axis of the cylinder in the direction of the external free stream for $Pe = 100$ and for $\gamma = 0.1$, 0.2, 0.5, 1, 2, 5 and 10

On the other hand, when γ is small, then the isotherms within the cylinder tend once again to concentric circles showing that the thermal field within the cylinder is almost independent of the external free stream. Figure 5 confirms that when γ is small then $\theta_c = \simeq 1/4(1 - r^2)$ at leading order. The numerical data used to plot Figure 6 also shows that the ratio of the interface temperatures at the upstream (forward) and downstream (rear) stagnation points tends towards roughly 0.3 as $\gamma \rightarrow 0$, which is an indication of the correction to the above leading order behaviour. Although, it is not obvious from Figure 6, the same ratio tends towards unity as γ becomes large.

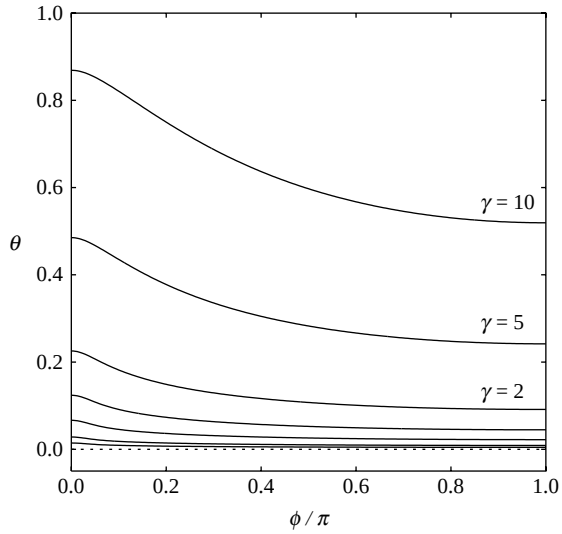

Figure 6.
Non-dimensional temperature profiles along the surface of the cylinder from the rear stagnation point at $\phi/\pi = 1$

Notes: The parameters are given by $Pe = 100$ and $\gamma = 0.1$, 0.2, 0.5, 1, 2, 5 and 10. The dashed line denotes the horizontal axis

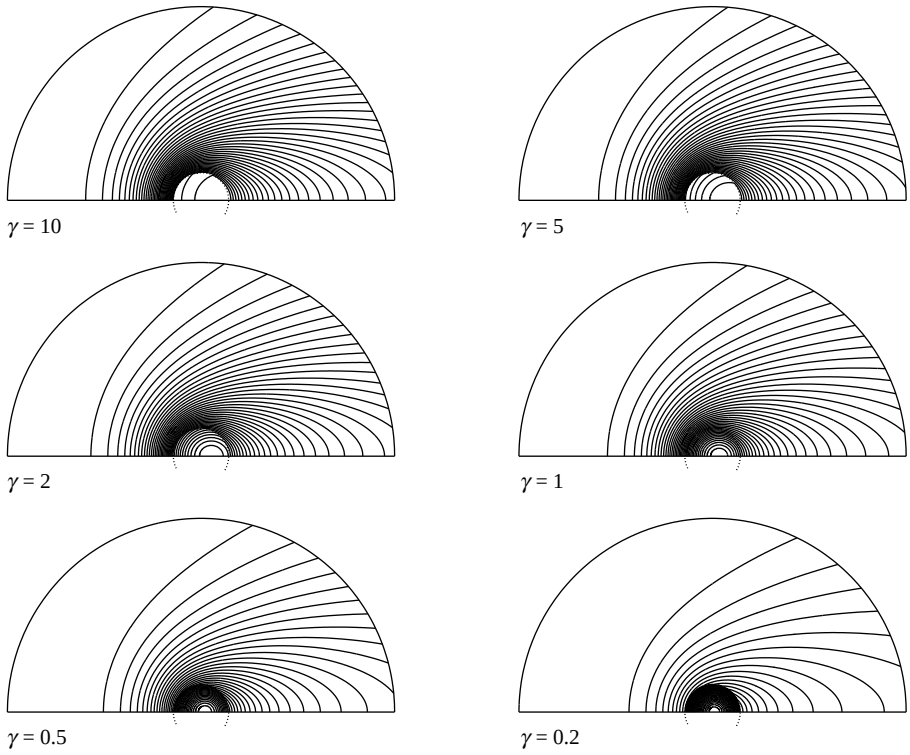

Figure 7.
the effect of different values of the conductivity ratio γ on the isotherms for $Pe = 1$

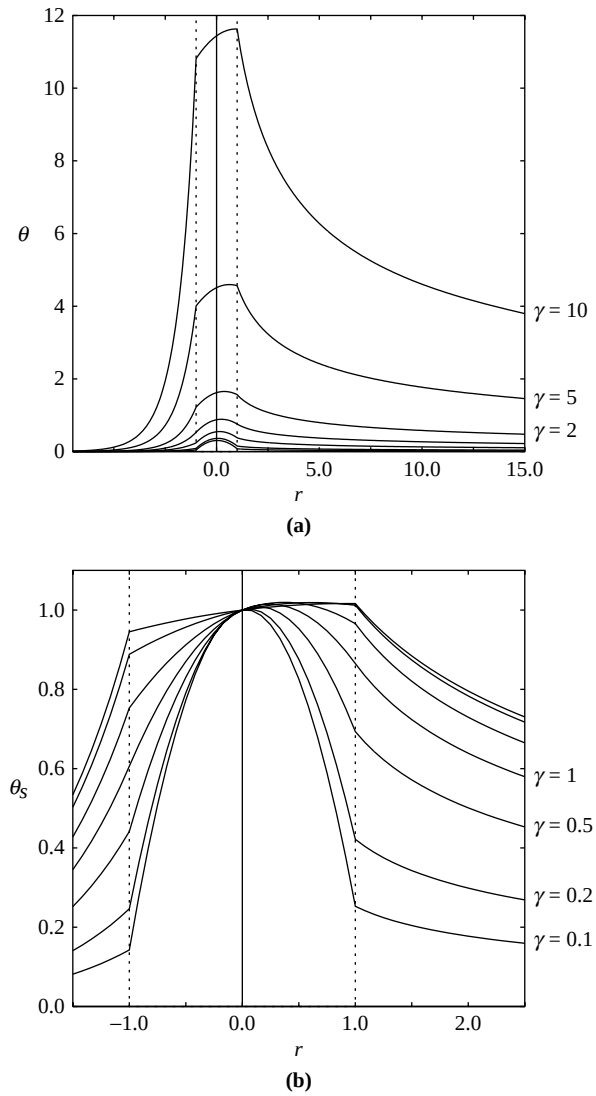

Notes: (a) computed temperature profiles; (b) scaled temperature profiles, θ_S

Figure 8.
Non-dimensional temperature profiles along the axis of the cylinder in the direction of the external free stream for $Pe = 1$ and for $\gamma = 0.1$, 0.2, 0.5, 1, 2, 5 and 10

The interface temperature profile when $\gamma = 100$, which is not shown in Figure 6 due to the magnitude of their values, 6.601 and 7.227, yields a ratio of roughly 0.91. Finally, it is necessary to point out that the overall shape of the external thermal field shown in Figure 4 varies little with γ. The apparent relative thickness of the wake region for $\gamma = 100$ as compared with the $\gamma = 0.1$ case is due to the fact that an equal number of isotherms are plotted in each case. When $\gamma = 100$ most of the temperature variation takes place within the porous medium, whereas the opposite occurs when $\gamma = 0.1$.

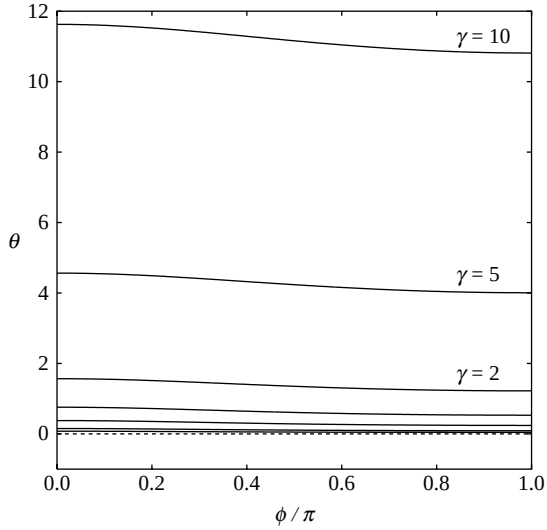

Figure 9.
Non-dimensional temperature profiles along the surface of the cylinder from the rear stagnation point at $\phi/\pi = 1$

Notes: The parameters are given by Pe = 100 and γ = 0.1, 0.2, 0.5, 1, 2, 5 and 10. The dashed line denotes the horizontal axis

When $Pe = 1$, the primary difference is that the thermal field in the porous medium is much more extensive than when $Pe = 100$, as may be seen when comparing Figures 7 and 4. As the external flow field is weaker, less heat is transported away from the cylinder by advection and therefore conductive effects are stronger. This effect may be shown in Figure 7 for $\gamma = 10$, for instance, where the thermal field within the cylinder is almost uniform, unlike the corresponding case for $Pe = 100$ shown in Figure 4. At $\gamma = 10$ the position of maximum temperature within the cylinder is almost exactly at the rear stagnation point; see Figure 8. Indeed, at such a low value of Pe there is little variation in the interface temperature, as may be seen in both Figures 8 and 9, and the maximum temperature attained is greater than for $Pe = 100$ due to the relative importance of conductive effects.

Conclusions

In this paper, we have sought to determine how conjugate heat transfer effects modify the forced convective heat transfer from a heated cylinder which is embedded within a porous medium. Heat is generated uniformly within the cylinder and the detailed isotherms and surface and axis temperature profiles have been found to depend strongly on the value of γ, which is the ratio of the conductivity of the cylidner to that of the porous medium. When seven is large, then there is little variation in temperature within the heated cylinder, and the temperature field within the porous medium approximates closely that here a fixed temperature is imposed on the surface of the cylinder. On the other hand, when γ is small, most of the temperature variation takes place within the cylinder, and we expect that the external temperature field, weak as it is, should correspond to that of a cylinder with a uniform heat flux imposed at the surface.

References

Bejan, A. and Kraus, A.D. (Eds) (2003), *Heat Transfer Handbook*, Wiley, New York, NY.

Bejan, A., Dincer, I., Lorente, S., Miguel, A.F. and Reis, A.H. (2004), *Porous and Complex Flow Structures in Modern Technologies*, Springer, New York, NY.

Ingham, D.B. and Pop, I. (Eds) (1998), *Transport Phenomena in Porous Media Vol. I*, Pergamon, Oxford.

Ingham, D.B. and Pop, I. (Eds) (2002), *Transport Phenomena in Porous Media Vol. II*, Pergamon, Oxford.

Ingham, D.B. and Pop, I. (Eds) (2005), *Transport Phenomena in Porous Media Vol. III*, Pergamon, Oxford.

Ingham, D.B., Bejan, A., Mamut, E. and Pop, I. (Eds) (2004), *Emerging Technologies and Techniques in Porous Media*, Kluwer, Dordrecht.

Kimura, S. (1988), "Forced-convection heat-transfer about an elliptic cylinder in a saturated porous-medium", *Int. J. Heat Mass Transfer*, Vol. 31, pp. 197-9.

Kimura, S. (1989), "Transient forced-convection heat-transfer from a circular-cylinder in a saturated porous-medium", *Int. J. Heat Mass Transfer*, Vol. 32, pp. 192-5.

Kimura, S. and Pop, I. (1992), "Conjugate free-convection from a circular-cylinder in a porous-medium", *Int. J. Heat Mass Transfer*, Vol. 35, pp. 3105-13.

Kimura, S. and Yoneya, M. (1992), "Forced convection heat transfer from a circular cylinder with constant heat flux in a saturated porous ediu", *Heat Transfer Japanese Research*, Vol. 21, pp. 250-8.

Kimura, S., Kiwata, T., Okajima, A. and Pop, I. (1997), "Conjugate natural convection in porous media", *Adv. Water Res.*, Vol. 20, pp. 111-26.

Kloker, M., Konzelmann, U. and Fasel, H. (1993), "Outflow boundary conditions for spatial Navier-Stokes simulations of transitional boundary layers", *AIAA Journal*, Vol. 31, pp. 620-8.

Nasr, K., Ramadhyani, S. and Viskanta, R. (1994), "An experimental investigation on forced-convection heat-transfer from a cylinder embedded in a packed-bed", *Trans. A.S.M.E.J. Heat Transfer*, Vol. 116, pp. 73-80.

Nield, D.A. and Bejan, A. (2005), *Convection in Porous Media*, 3rd ed., Springer, Berlin.

Pop, I. and Ingham, D.B. (2001), *Convective Heat Transfer: Mathematical and Computational Modelling of Viscous Fluids and Porous Media*, Pergamon, Oxford.

Pop, I. and Nakayama, A. (1999), "Conjugate free and mixed convection heat transfer from vertical fins embedded in porous media", in Sunden, B. and Heggs, P.J. (Eds), *Recent Advances in Analysis of Heat Transfer for Fin Type Surfaces*, Computational Mechanics Publications, Southampton, pp. 67-96.

Pop, I. and Yan, B. (1998), "Forced convection flow past a circular cylinder and a sphere in a Darcian fluid at large Péclet numbers", *Int. Comm. Heat Mass Transfer*, Vol. 25, pp. 261-7.

Rees, D.A.S., Bassom, A.P. and Pop, I. (2003), "Forced convection past a heated cylinder in a porous medium using a thermal nonequilibrium model: boundary layer analysis", *Eur. J. Mech. B-Fluids*, Vol. 22, pp. 473-86.

Vafai, K. (Ed.) (2000), *Handbook of Porous Media Vol. I*, Marcel Dekker, New York, NY.

Vafai, K. (Ed.) (2005), *Handbook of Porous Media Vol. II*, Marcel Dekker, New York, NY.

Vaszi, A.Z., Elliott, L., Ingham, D.B. and Pop, I. (2003), "Conjugate free convection from vertical fins embedded in a porous medium", *Num. Heat Transfer, Part A*, Vol. 44, pp. 743-70.

Vaszi, A.Z., Elliott, L., Ingham, D.B. and Pop, I. (2004), "Conjugate free convection from a vertical plate fin with a rounded tip embedded in a porous medium", *Int. J. Heat Mass Transfer*, Vol. 47, pp. 2785-94.

Wong, W.S., Rees, D.A.S. and Pop, I. (2004), "Forced convection past a heated cylinder in a porous medium using a thermal nonequilibrium model: finite Péclet number effects", *Int. J. Thermal Sci.*, Vol. 43, pp. 213-20.

Corresponding author
D.A.S. Rees can be contacted at: ensdasr@bath.ac.uk